Nonlinear Dyn (2024) 112:11471–11481
https://doi.org/10.1007/s11071-024-09671-z

RESEARCH

Hardware implementation of the ring generator with tunable frequency based on electronic neurons

Nikita M. Egorov · Marina V. Sysoeva · Maksim V. Kornilov · Vladimir I. Ponomarenko · Ilya V. Sysoev

Received: 13 February 2024 / Accepted: 25 April 2024 / Published online: 23 May 2024

Abstract Constructing electronic models of neurons has several goals. First, it aims to reproduce the dynamics of biological neurons and their networks (simulation). Second, the resulting networks can be used for neuroprosthetics. In the brain, most neurons themselves are in a non-oscillatory mode, and brain rhythms arise due to their collective dynamics. In this case, very small ensembles of neurons can act as rhythm generators. Such ensembles can be constructed and studied within the framework of a electronic experiment. In this work, a circuit of several (from eight to fifteen) FitzHugh–Nagumo electronic oscillators with electronic synapses (sigmoid coupling function and delay were implemented) was constructed. Oscillatory modes were realized in this circuit as a result of collective dynamics, with their frequency being controlled with changing a delay in the synapse and/or altering the number of elements in the ring. The oscillatory modes coexist with a stable fixed point and may be activated by means of short time external driving. Thus, the presented generator is capable of well reproducing both a slowly gradual change in the main oscillation frequency and its sharp change, with both of these phenomena well diagnosed from time series of brain local field potentials at limbic epilepsy.

Keywords FitzHugh–Nagumo neuron · Electronic ring generator · Sigmoid coupling · Time delayed systems · Tunable frequency · Central rhythm generator

N. M. Egorov · M. V. Sysoeva · M. V. Kornilov · V. I. Ponomarenko · I. V. Sysoev (✉)
Saratov Branch of the Institute of Radioengineering and Electronics of Russian Academy of Sciences, 38, Zelyonaya str., Saratov, Russia 410019 ·
N. M.Egorov
Yuri Gagarin State Technical University of Saratov, 77, Politekhnicheskaya str., Saratov, Russia 410054 ·

M. V. Sysoeva · M. V. Kornilov · V. I. Ponomarenko · I. V. Sysoev
Saratov State University, 83, Astrakhanskaya str., Saratov, Russia 410012
e-mail: ivssci@gmail.com

1 Introduction

Construction of models reproducing behavior of real neurons and their ensembles is of both scientific and technical interest. In particular, the concept of a central rhythm generator is actively developing in robotics [1–3]. In particular, the main rhythm is necessary for realization of simple movements which are characteristic of living organisms. When modeling pathological regimes of brain functioning, including epilepsy, the mechanisms of basic rhythm generation is also of a high importance. Here, we attempt to describe the occurrence and evolution of the main oscillation frequency in the hippocampus at limbic epilepsy (see the modern epilepsy classification in [4]) using a small number of electronic oscillators constructed from physiological reasons and connected in a ring. The main biological basis we use was obtained from rat models [5,6]. Compared with purely mathematical model-

ing, electronic implementation allows us to approach a biological experiment closer by a number of criteria: specifics of measurements, non-stationarity of the circuit parameters, non-identity of circuit elements. At the same time, models using microcontrollers such as Arduino [7] are another (next to SPICE simulators) intermediate link between fully analog modeling and numerical solution of equations.

Earlier in the paper [8], a hardware implementation of a simplified FitzHugh–Nagumo neuron with one bifurcation parameter was proposed. The SPICE–model consisting of 14 simplified FitzHugh–Nagumo neurons connected with a simple linear coupling was constructed in [9]. In [10], it was demonstrated that such SPICE–model successfully scales and reproduces the inherent variability of biological systems, including variety in the number of elements and in the coupling architecture. As a result, eight connectivity configurations of 14 simplified FitzHugh–Nagumo neurons were implemented [11]. The radio engineering experiment showed that the implemented circuits are able to demonstrate the desired behavior—long-term quasi-regular transients reproducing various characteristics of epileptiform activity at absence epilepsy, following what had been previously shown in mathematical modeling [12,13]. Further, a circuit of a complete FitzHugh–Nagumo neuron with two bifurcation parameters a and b and a circuit of a chemical synapse mathematically representing a sigmoid function were developed in [14]. In [15] it was shown that in two hardware complete FitzHugh–Nagumo neurons connected with a sigmoid couplings, different scenarios of oscillation occurrence were possible, including saddle-node cycle bifurcation leading to appearance of highly nonlinear limit cycles of large amplitude. Long-living transients were detected near these bifurcations.

The delay naturally occurs in the synapse when a signal is transmitted between the axon and the dendrite as a result of the finiteness of the ion transport speed. It may have a significant impact on the network dynamics [16]. Theoretically, impact of the delay on the dynamics of two coupled FitzHugh–Nagumo neurons with chemical synapse was studied in [17]. So, the model used previously was improved by adding a delay in the coupling [18]:

$$\begin{aligned}\varepsilon\dot{u}_i(t) &= u_i(t) - c_i u_i^3(t) - v_i(t) \\ &\quad + \sum_{j\neq i} k_{ij} h\left(u_j(t-\tau)\right), \\ \dot{v}_i(t) &= u_i(t) + a_i - b_i v_i(t), \\ h(u) &= \frac{1+\tanh(u)}{2}, \end{aligned} \tag{1}$$

where u is a dimensionless variable corresponding to the transmembrane potential in a biological excitable tissue; v is a dimensionless variable similar to slow recovery current; t is dimensionless time; ε is an inertia parameter; a and b are dimensionless parameters that control the neuron own dynamics; c is an integration constant (usually $c = 1/3$); k is a coupling coefficient, while the coupling is implemented in the form of an offset hyperbolic tangent h; τ is time delay.

Four variants of tunable analog delay were compared in [18]. The standard "DELAY" component from the National Instruments Multisim electronic circuit simulator was used as a reference. We also considered a first-order all-pass filter with a potentiometer, a Bessel filter with a potentiometer, and sequentially connected Bessel filters, each of which simulates a fixed delay time. As a result, it was decided to focus on one Bessel filter with a potentiometer as a preferable implementation. The SPICE–circuit of a ring generator consisting of 20 neurons with improved synapses was created in [18]. The key feature of this generator was that its frequency could be changed in three different ways: by changing the delay time (smooth tuning is available in a wide range), by changing the number of elements in the network (frequency tuning is carried out stepwise), by varying the frequency of an external driving (under conditions of multistability, coexisting regimes with multiple frequencies can be realized).

The purpose of this work is to construct the hardware implementation of a ring generator, the theoretical study of which was performed in [18].

2 Analog generator

A circuit diagram of the complete FitzHugh–Nagumo electronic oscillator with synapse is shown in Fig. 1. In contrast to the mathematical model, see Eq. (1), the parameters of the electronic circuit have dimensions. Therefore, there are two time-scale parameters: $E = R11C1$ and $T = R7C2$. The parameter ε from Eq. (1) is calculated as $\varepsilon = E/T$. The parameters $c = (R3 + R4)/R3$ and $b = R6/\left(R5 + R_b \cdot \frac{B}{100\%}\right)$ (to set B percentage of the potentiometer R_b was used) are scaling factors at U and V respectively, which are dimensional analogs of two variables of the mathemat-

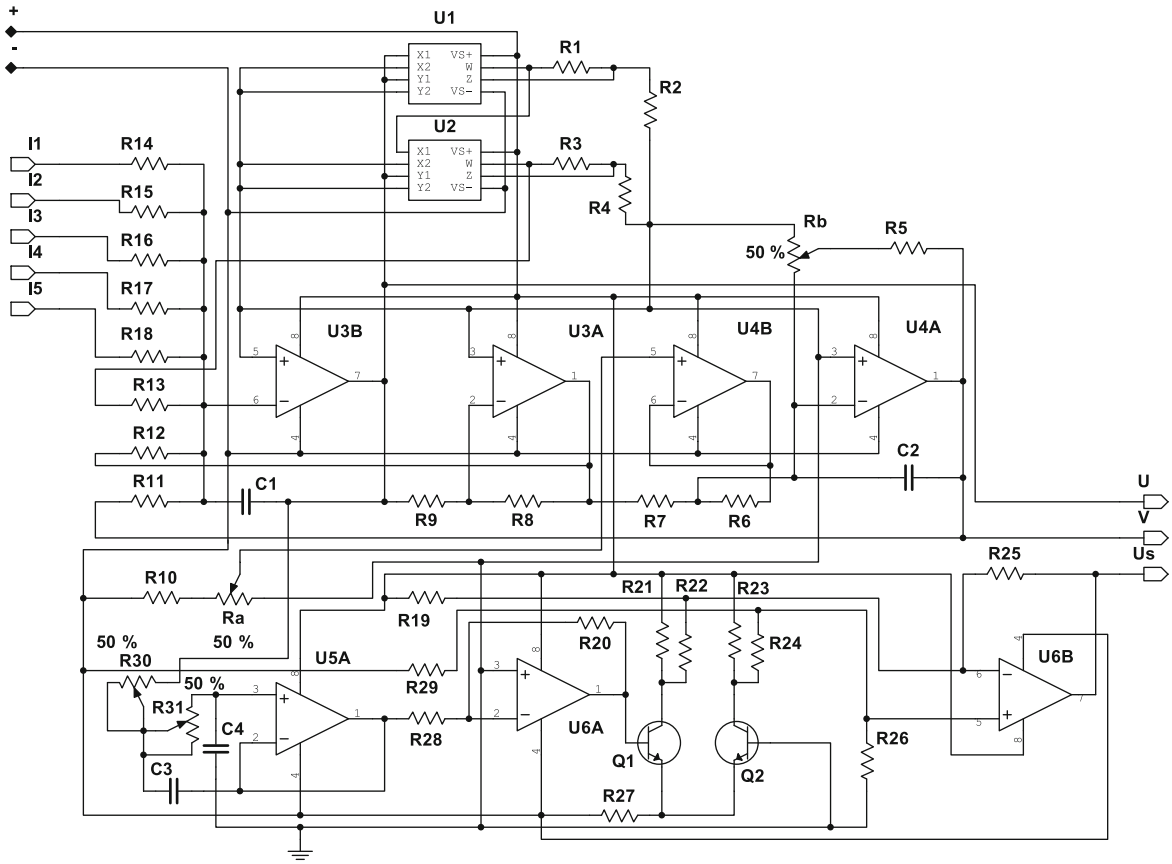

Fig. 1 Circuit diagram of a single complete FitzHugh–Nagumo neuron with a synapse. Parameters of the neuron: $R1 = R3 = 1\,\text{k}\Omega$, $R2 = 9\,\text{k}\Omega$, $R4 = 2.333\,\text{k}\Omega$, $R5 = 51\,\text{k}\Omega$, potentiometer $R_b = 4.7\,\text{M}\Omega$, $R6 = R7 = R8 = R9 = R11 = R12 = R13 = 100\,\text{k}\Omega$, $R10 = 5\,\text{k}\Omega$, potentiometer $R_a = 1\,\text{k}\Omega$, $R14 - R18$ depends on coupling strength k, $C1 = 1$ nF, $C2 = 0.01$ uF, U1, U2 are multipliers of the type AD633, and U3, U4 are amplifiers of the type AD822. Parameters of the delay in the form of a Bessel filter with potentiometers: $R30 = R31 = 50\,\text{k}\Omega$, $C3 = 5.6$ nF, $C4 = 3.9$ nF, U5A is an amplifier of the type LM358AD. Paramters of the synapse (sigmoid function): $R19 = R29 = 300\,\text{k}\Omega$, $R20 = 0.51\,\text{k}\Omega$, $R21 = R23 = 1\,\text{k}\Omega$, $R22 = R24 = R28 = 10\,\text{k}\Omega$, $R25 = R26 = 5.1\,\text{k}\Omega$, $R27 = 2\,\text{k}\Omega$, Q1, Q2 are bipolar junction transistors of the type 2N1711, U6 is an amplifier of the type NE5532AI. There are three outputs in the circuit: U and V (both used for measurement and corresponding to the model u and v variables) and Us, corresponding to the synaptic output $h(u)$

ical model u and v in the Eq. (1). Coupling coefficient k is calculated as $k = R13/R_{\text{IN}}$, where R_{IN} is the nominal value for one of the input resistors from $R14$ to $R18$. The parameter a is set by the voltage at the "+" clamp of the amplifier U4B. The total voltage drop on a series-connected resistor $R10 = 5\,\text{k}\Omega$ together with a potentiometer $R_a = 1\,\text{k}\Omega$ is $U_a = 15$ V, i. e. the voltage drop on the entire potentiometer is 2.5 V. In particular, if the potentiometer is set to $A = 0\%$, the voltage 2.5 V is set to "+" input of U4B, and if the potentiometer is set to $A = 100\%$, this voltage is zero. So, the parameter a can be calculated using A measured in percents of potentiometer resistance as follows: $a = 2.5 \cdot \left(1 - \frac{A}{100\%}\right)$.

The circuit for one neuron contains two analog multipliers U1 and U2 and two dual operational amplifiers U3 and U4. Elements U3B and U4A are integrators. They allow to obtain U and V, respectively. Element U3A is an inverter. It allows to obtain $-U$. Element U4B is a repeater. The amplifiers U1 and U2 perform the cubic transformation according to the formula (1).

The chemical synapse circuit consists of two parts: a circuit simulating an analog delay, and a circuit implementing a sigmoid function (electronic implementa-

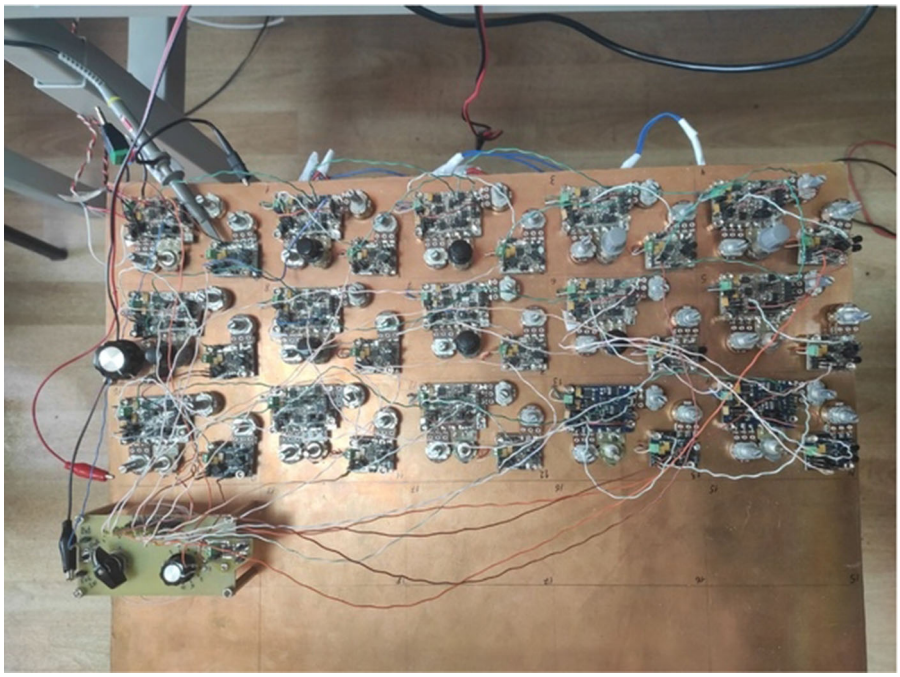

Fig. 2 Photograph of the hardware implementation of a neuron-like activity electronic ring generator with a tunable frequency. There are 15 neurons N1–N15 with synapses in three rows, five in a row. The pontentiometer used to set the value of a_{ring} is located at the left bottom of the photograph

tion of a hyperbolic tangent). The first circuit contains a second-order Bessel filter based on the operational amplifier U5A. The second circuit contains a dual operational amplifier U6 and two bipolar transistors Q1 and Q2. The inverting amplifier U6A has a gain of 0.05, the differential amplifier U6B has a gain of 0.5.

The physical implementation of the ring generator consists of 15 neurons with synapses N1–N15, see Fig. 2. All neurons were connected in a ring unidirectionally, see Fig. 3. The neurons are set to be in a subthreshold mode with parameters $a_{\text{ring}} = 1.1$ and $b_{\text{ring}} = 0.09$, in this mode they may respond by a pulse to an external pulse, but do not generate any oscillatory activity by themselves. The external input is in an oscillatory mode with parameters $a_{\text{input}} = 0.875$ and $b_{\text{input}} = 0.08$. Driving from it is provided, if necessary, by pressing the button (bottom right in the Fig. 2). The coupling strength inside the ring and the coupling strength of external input were taken to be the same $k_{\text{ring}} = k_{\text{input}} = 1.0$. The number of neurons in the ring varied by means of the rotary switch from one to eight discretely.

When neurons are closed in a ring, a coupling occurs between them with a time delay, which corresponds to a delay in a chemical synapse in a real biological neuron caused by a finite times required for ion transport through the synapse. As a result, an oscillatory attractor can form in the ring, while a separate neuron has a single attractor in the form of a stable point. However, this oscillatory attractor often coexists with a stable equilibrium position, since it arises rigidly, not due to the Andronov–Hopf bifurcation, but as a result of the saddle-node bifurcation of the cycle [19,20] (in the two-dimensional case — this bifurcation is known as a birth of a cycle from the condensation of phase trajectories [21]). This mechanism for mathematical models of FitzHugh–Nagumo neuron networks was studied in [13], but without delay. It is responsible both for the formation of the attractor and for long-term transients occurring near the bifurcation point. Possibility of approaching this attractor depends on the initial conditions, for example, whether an electronic key is closed, or can be carried out by a short-term external driving. In this case, the model can go through a bifurcation of the birth (or death) of a cycle directly during the experiment due to changes in the parameters of electronic neurons because of heating.

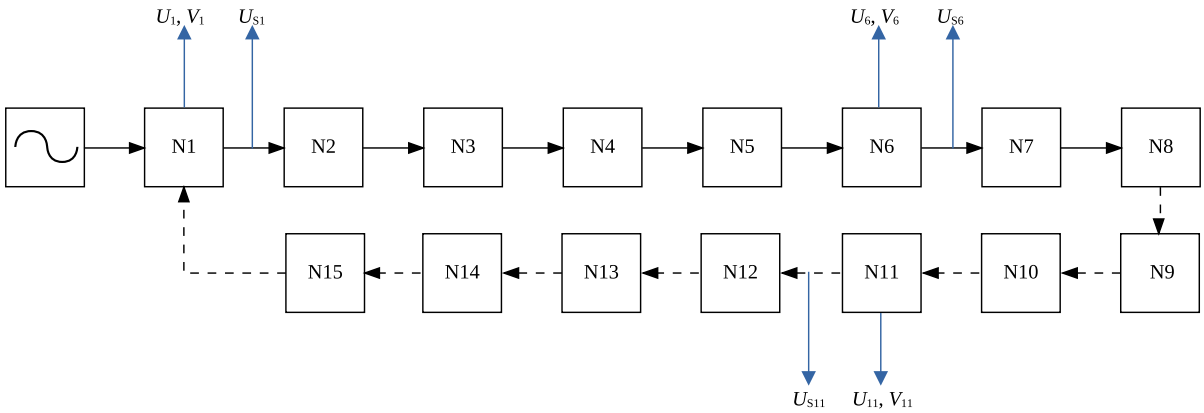

Fig. 3 Scheme of connection of neurons in the ring. Solid lined are for connection between first 8 neurons which are always in the ring, dashed lines are for additional neurons which may be included in the ring to change the oscillation frequency. Sine symbol shows the signal generator used to initiate oscillations in the ring (to switch between attractors). The places in the circuit from which the signals were measured are shown with blue arrows

3 Experimental results

3.1 Procedure of recording

Data were recorded with an analog-digital converter LCARD E14-140 M (Russia) with the following characteristics: number of channels—up to 32, sampling frequency $f_s = 200$ kHz for all channels, quantization bit length—14 bits, dynamical range—± 10 V. There were different types of recordings. Most experiments were recorded in two-channel regime with sampling frequency 100 kHz per channel. First, we recorded variable U from two neurons, mostly N1 and N5. This was done to detect that all neurons behave similarly and that phase shift between neurons in the ring is determined by the distance between them. Next, we recorded dynamics of one neuron: both variables U and V. We also combined these two types of experiments to record U and V from two neurons together with sampling frequency 50 kHz. Additionally, we recorded the postsynaptic voltage Us together with presynaptic variable U in some preliminary experiments in all neurons in order to control realization of the synapse (hyperbolic tangent function).

The parameters of the circuit were set to $a = -1.2$, $b = 0.08$, which corresponded to a stable focus attractor in a single uncoupled neuron. At the beginning of the experiment there were no oscillations in the circuit. Oscillations in the ring were excited via short in time external harmonic driving of the amplitude 0.5 V with the offset -0.5 V (oscillation range $[-1; 0]$ V) with the frequency 200 Hz, which was applied to the inverted input of the neuron N1. JUNTEK PSG9080 (China) programmable signal generator was used to generate the driving. This driving started by button press and lasted for 5–20 periods (25–100 ms). The alternative way to switch between attractors (from table point to the limit cycle) was implemented for smaller (11 and less neurons) networks by using one of the neurons as an external driving instead of the generator of harmonic oscillations; in this case the parameters of this single neuron were set to $a = 0.8, b = 0$, which corresponded to a periodic regime. Both excitation approaches led to the same regular autonomous dynamics (short in time transient nonautonomous regimes under external driving were not considered).

3.2 Time series and phase plots

Time series of the neuron N1 at the parameters $\tau = 0.5$ ms, $D = 15$, $k = 0.6$ were plotted on the Fig. 4a, and the phase plot on the plane (U, V)—on the Fig. 4b. The oscillation form and amplitude are typical for all achieved regimes. One also can see that pulses (especially for U variable) are not completely identical. The variation of the signal shape is determined by two main factors. First, there is evolution of parameters of semiconductor elements due to heating. Second, there are significant real differences in parameters between neu-

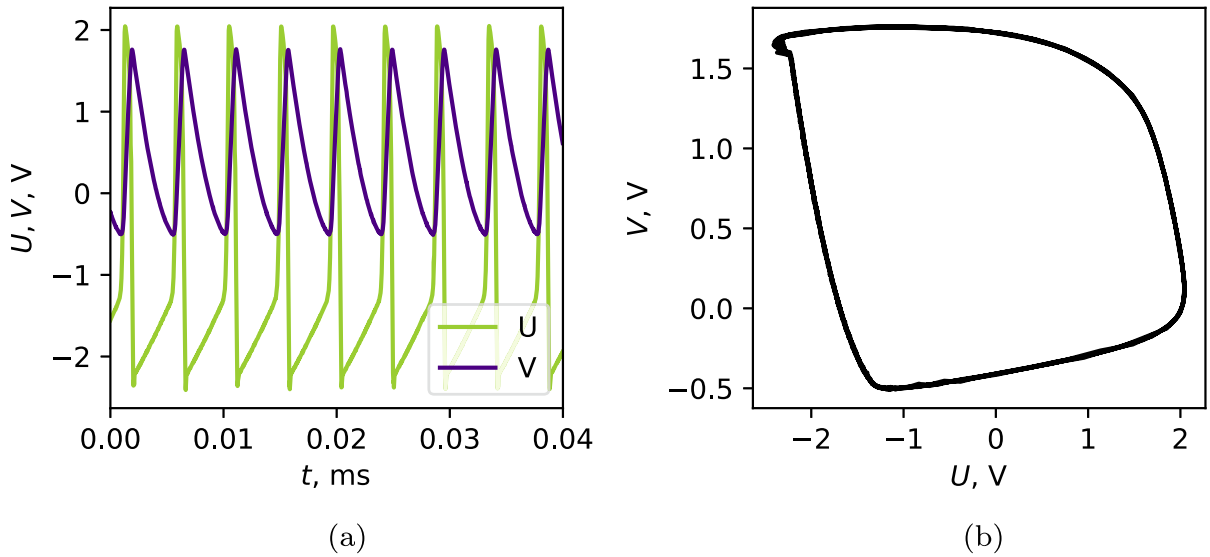

Fig. 4 Time series of variables U and V (**a**) and phase plot (**b**) for the neuron N1 at the parameters $\tau = 0.2$ ms, $D = 15$, $k = 0.6$

rons. These two factors lead to continuous "synchronization" (lag-synchronization) process between neurons in the network. This "synchronization" is not a classical synchronization described in [22,23], which is leading to adjustment of oscillation rhythms of two or more coupled systems, since in our case each node of the ring is in the non-oscillatory mode by itself. But if we consider the ring without a single considered node as a generator, this incomplete ring may be thought to synchronize the considered node in the terms of forced synchronization. Let us consider another interpretation. If we consider the ring of identical oscillators as it was studied theoretically in [24] and other similar works and replace one of them by an oscillator with somewhat different parameters, the dynamics of this oscillator will be synchronized by the ring.

The effective difference in the neuron parameters is distinguishable, see Fig. 5, where the series of three neurons: N1, N6 and N11 were plotted for $D = 15$, $\tau = 0.5, k = 1.0$ (series of U and V for these 3 neurons were measured with the sampling frequency 25 kHz). In the Fig. 5a one can see that the time distance between maxima of U for three considered neurons is close to $T/3$, where $T = 1/f = 5.96$ ms. In the Fig. 5b the pulse of N11 is just preceding the pulse of N1, with oscillation period being smaller $T \approx 4.4$ ms. There are also differences between neuron shape for $D = 15$ (Fig. 5a) and $D = 11$ (Fig. 5b): for the regime with the smaller frequency there is an additional minimum at the period (neurons have enough time to relax after the stimulus).

3.3 Generator frequency as it depends on ring size and delay time

Based on experiments done for all possible combinations of $1 \leqslant D \leqslant 15$ and $\tau \in \{0.1, 0.2, 0.3, 0.4, 0.5\}$ ms we constructed the dependencies of the main oscillation frequency f on the number of elements in the ring D and on the delay time τ. These dependencies were plotted in Fig. 6. Study was performed for two different values of k: $k = 0.6$—see Fig. 6a and $k = 1.0$—see Fig. 6b. These two diagrams are mostly similar with the following differences:

- the frequencies for $k = 1.0$ are somewhat larger than for $k = 0.6$, this was the case for every D and τ for which the oscillatory activity in the ring was possible;
- there is an oscillatory regime for $\tau = 0.2$ ms and $D = 11$ for $k = 0.6$ ms which is absent for $k = 1.0$.

Speaking in terms of lag-synchronization, we may note that increasing k leads to reduce of lag.

The dependency of the main frequency f of oscillations on D and τ plotted in Fig. 6 may be approximated by a hyperbolic function, as it was done for model ring consisted of Hodgkin–Huxley neurons in [25]. To make the approximation problem linear let us

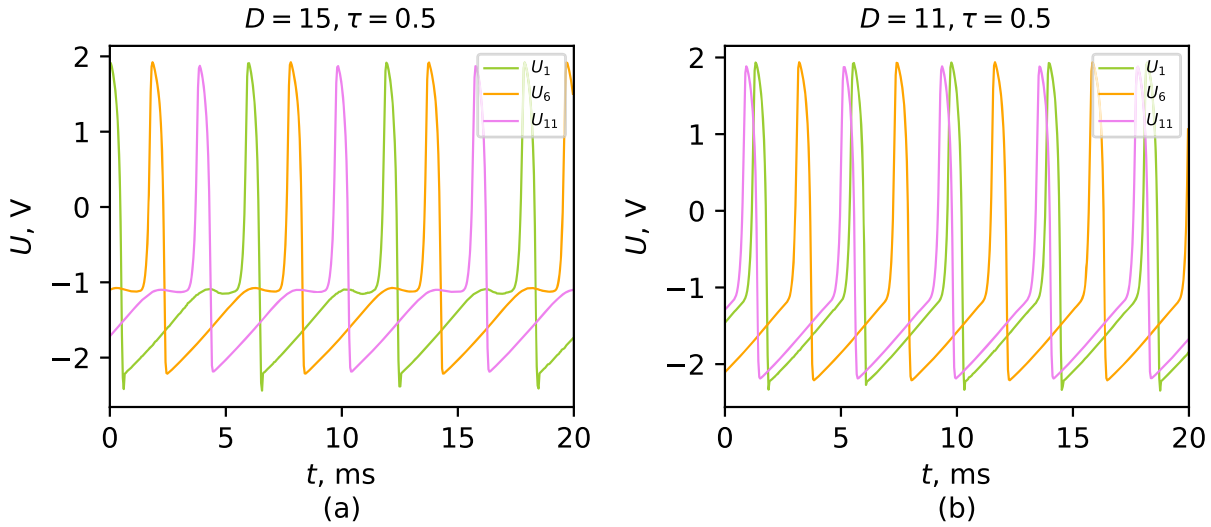

Fig. 5 Time series of U variable for three neurons: N1, N6 and N11 for $\tau = 0.5$ and different numbers of neurons: $D = 15$ (**a**) and $D = 11$ (**b**), $k = 1.0$ for both subplots

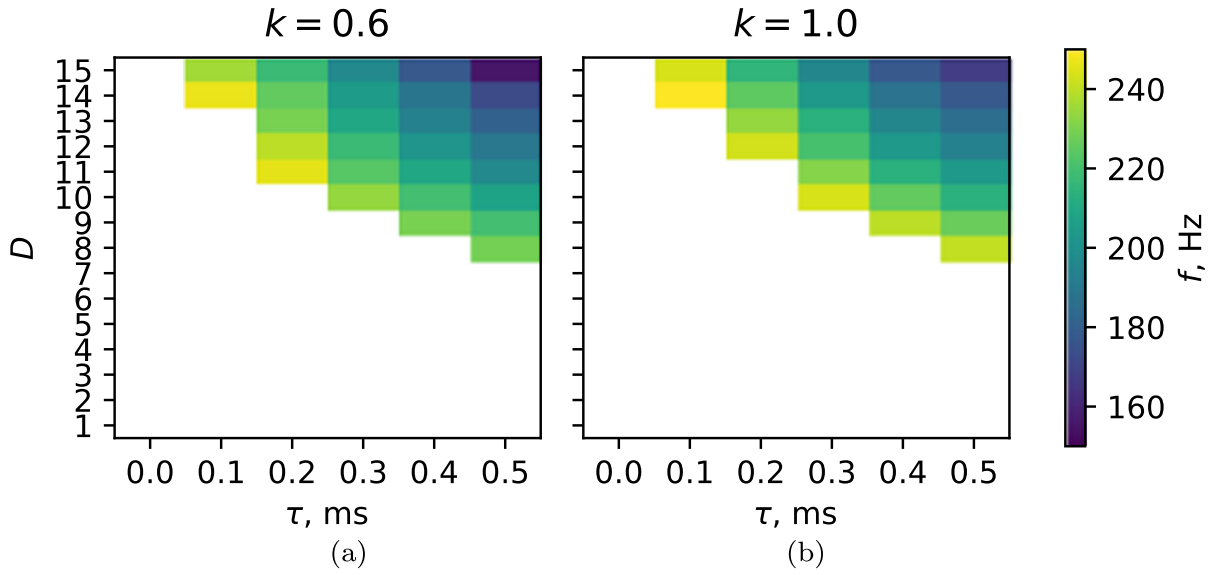

Fig. 6 Dependencies of the main oscillation frequency f in the circuit on the number of elements in the ring D and on the delay time τ: **a** before the driving; **b** after the driving. The color indicates the oscillation frequency occurring in the ring

consider dependence of the oscillation period $T = 1/f$ rather than frequency. Following [25] let us consider the following dependency:

$$T_{\text{fit}}(D, \tau, k) = T_0(k) + \gamma(k)\tau D + \varepsilon(k)D, \tag{2}$$

where $T_{\text{fit}} = 1/f_{\text{fit}}$ is the approximation of the period T measured experimentally, T_0, ε and γ are constants, depending only on k, with T_0 and ε having the dimension of time and γ being dimensionless. The parameter ε can also be considered as a parameter of inertia of a single neuron.

We fitted the parameters T_0, ε and γ to experimental data for both considered $k = 0.6$ and $k = 1.0$ separately. All frequency values obtained in each experiment ($Z = 27$ for the experiment with $k = 0.6$ and $Z = 28$ for the experiment with $k = 1.0$) were used for this fitting at once. The results together with a relative

Table 1 Values of the parameters T_0, ε and γ in the formula (2) fitted for different k with the mean squared normalized error of approximation σ^2_{appr}

k	T_0, ms	γ	ε, ms	σ^2_{appr}
0.6	2.35	$3.22 \cdot 10^{-4}$	0.088	0.0193
1.0	2.13	$3.01 \cdot 10^{-4}$	0.106	0.0077

mean squared approximation error (3) are shown in the Table 1.

$$\sigma^2_{\text{appr}} = \frac{1}{Z} \sum_{D=8}^{15} \sum_{\tau=\tau_{\min}}^{\tau_{\max}} \left(f_{\text{exp}} - f_{\text{fit}}\right)^2, \tag{3}$$

where Z is the total number of pairs τ and D for which oscillatory regime was reachable ($Z = 28$ for $k = 0.6$ and $Z = 27$ for $k = 1.0$), $\tau_{\max} = 0.5$ and $\tau_{\min}$ is different for different D and k, see Fig. 6 for details.

Based on the values of approximation error we may conclude that the analytical formula (2) pretty well describes the results of the experiment, though for the mathematical model considered in [25] this errors was 10 times smaller. The particular values for experimentally observed frequency and its approximation are given in the Fig. 7 (we plotted only part of values as dependencies on τ for the maximal used $D = 15$ and on D for the maximal used $\tau = 0.5$ ms). The differences between the formula and the experiment seem to be caused by nonidentity of neurons and synapses. The most noticeable differences between measured and fitted frequency values correspond to the smallest frequencies at the the boundary of oscillatory mode on the parameter plane (D, τ), with experimental values being usually smaller than fitted ones. Regimes at the boundary of the oscillation region are most vulnerable to non-identity of network elements and are the first to collapse or distort. This could at least partly explain larger errors of fitting for these regimes.

However, in general the approximation shows that for a certain chosen value of k the generator frequency may be well predicted and calculated for given D and τ if one has at least three measurements for different D and τ values to estimate the parameters T_0, ε and γ.

4 Conclusion and discussion

The novelty of this study is as follows. First, the electronic model of an individual neuron was taken from [15], but a delay was introduced in the coupling, which simulates a real delay in a chemical synapse. The delay was implemented in the form of a tunable Bessel filter, where one of the resistors was replaced by a potentiometer. The delay in the synapse significantly expands the set of modes which can exist in a network of coupled electronic neurons. Theoretically, very similar system of two neurons was studied in [17], but Heviside's function was used to approximate the synapse instead of sigmoid. Second, while developing the scheme, we succeeded to reproduce the results of previous work on mathematical [26] and SPICE [18] modeling. We aimed to obtain a specific mode of behavior in a unidirectionally coupled ring of neurons, in which the frequency of periodic pulse oscillations is controlled by a delay in couplings and depends on the number of elements and coupling coefficient k, which was set by a potentiometer. This was achieved for sufficiently large delay values for eight or more neurons: in total, in 28 different combinations of the number of elements D and delay time τ for $k = 0.6$ and 27 for $k = 1.0$. There was also possible to obtain oscillatory regimes for even smaller coupling $k \gtrsim 0.4$. We have shown that at this specific coupling architecture at least two stable regimes (fixed point and periodic attractor) coexist, with switching between them being possible via short in time external driving of various type and length. Third, we have performed an approximation of the law according to which the frequency of generation depends on the number of neurons and the coupling delay time at the given k. This approximation showed that the law written in [25] for the ensemble of mathematical Hodgkin–Huxley neurons is able to describe the similar dependency for electronic FitzHugh–Nagumo neurons in a real world experiment and is likely to be universal.

From our point of view, the hardware implementation of neurons has exactly that main advantage over the mathematical modeling, which allows us to partially reproduce the difficulties inherent in the study of biological neurons. All neurons and synapses in the electronic circuit are not identical in parameters (this led to some differences in signal shape), they do not perfectly repeat the mathematical model, their parameters change over time, including due to heating. Therefore, the fact of detection of the desired modes indicates the great structural stability of the proposed generation mechanism. This means that in a biological system, where the role of non-identity and non-stationarity is even greater, one can still expect to observe such

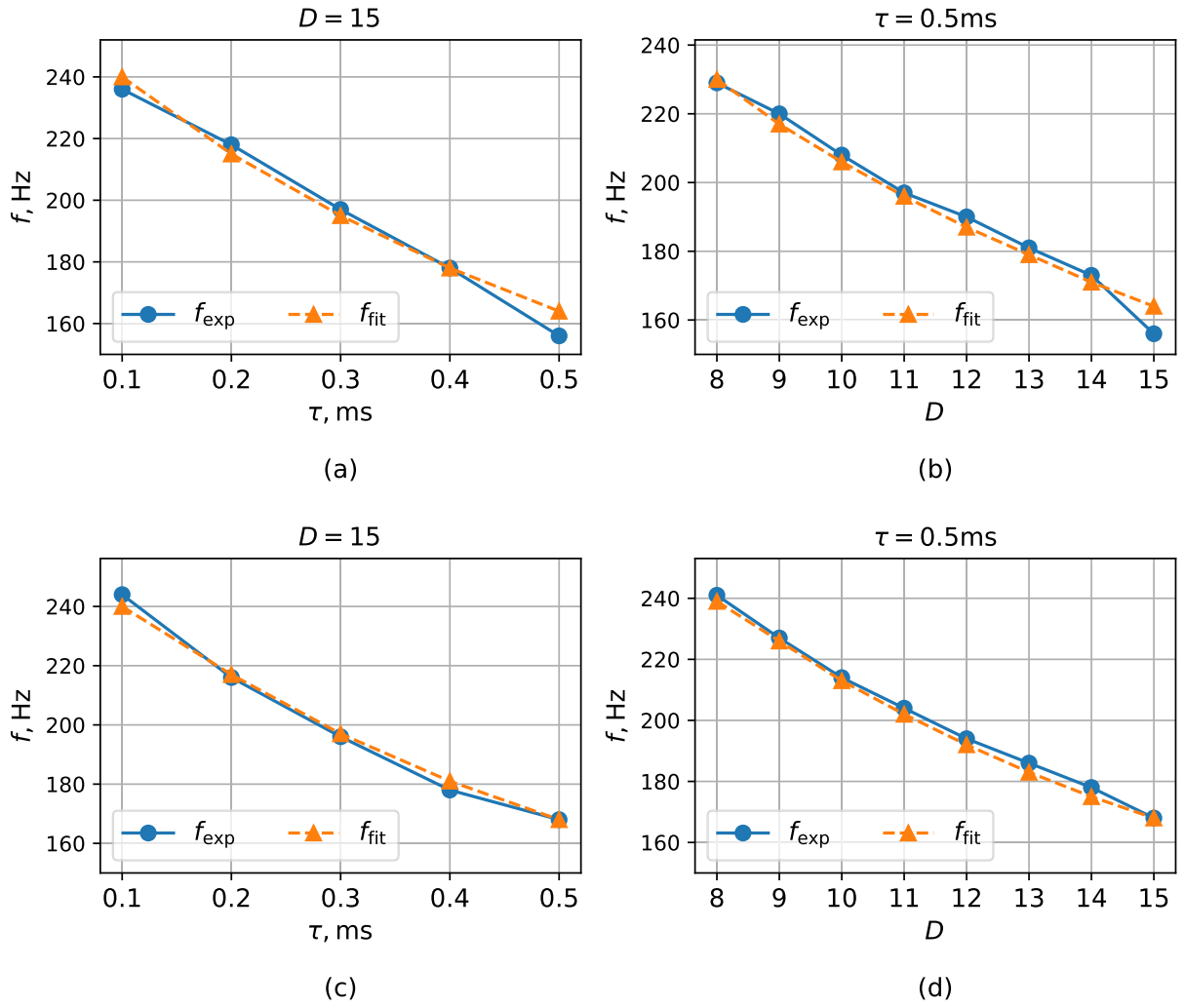

Fig. 7 Experimentally observed f_{exp} (cyan) and approximated f_{fit} (orange) values of the generation frequency for different values of k: subplots (**a**) and (**b**) correspond to $k = 0.6$, subplots (**c**) and (**d**) correspond to $k = 1.0$. Subplots (**a**) and (**c**) were constructed for the same value of $D = 15$ and different τ, subplots (**b**) and (**d**) were constructed for the same $\tau = 0.5$ ms and different values of D

modes. The role of the studied regimes can be very great for the formation of the limbic epilepsy basic rhythm. According to modern concepts, a very small network of hippocampal neurons can be responsible for it [27]. In contrary to microscopic silicon implementations of neurons [28,29] which are preferred if a large ensemble is desired, the parameters of the macroscopic models [8,15,30] can be well controlled. This makes possible specifying parameters for a particular neuron type: for pyramid neurons and interneurons of neocortex and hippocampus, thalamoctical neurons and reticular thalamic nucleus neurons, which is valuable for microcircuit modeling and would be a next step in modeling both limbic and thalamocortical brain systems.

In limbic epileptic seizures, the oscillation frequency can change both smoothly [31] and abruptly [32]. In the presented model, these two ways of frequency evolution are reproduced by smooth changing the resistance of the potentiometer and decreasing/increasing the number of neurons in the network by switching the electronic key correspondingly. However, the constructed generator may be useful regard-

less of its biological prototype as a source of multi-frequency periodic pulse signals.

The number of neurons examined in this study increased 7.5 times compared to [15]. This shows the scaling capabilities of the circuit proposed in [15]. Since the complexity of implementation and consideration of all possible coupling architectures within the single work would be excessive, we limited ourselves to studying only one coupling architecture (unidirectional ring), which is very important from physiological reasons.

Compared to earlier studies [8,11], in the present experiment all synaptic couplings were analog devices rather than microcontroller based connections using digitized signals; in [30] the coupling was also analog, but it was linear and therefore not synaptic-like. The synaptic analog coupling, on the one hand, is much more complicated for implementation. But on the other hand, such an implementation is much closer to biological experiment. The possible next step is switching from hardware realization of FitzHugh–Nagumo model to the Morris–Lecar like model which is known as a simplest biologically proven model (some first implementation of which was published in [33]).

Author contributions N.E. and M.S. developed and constructed the hardware setup, they also measured signals. V.P. proposed some technical solutions for setup construction and wrote the experimental part of the manuscript together with M.S. M.K. realized approximation of the experimental frequency (analytical formula fitting) and wrote the corresponding subsection. I.S. proposed the idea of setup and wrote introduction, results (together with M.S. and M.K.) and conclusion. N.E. made Fig. 1 and 3, M.S. made Fig. 2, I.S. made Figs. 4–6, M.K. made Fig. 7. I.S. and V.P. revised the manuscript and wrote answers to reviewers, M.K. reworked Fig. 7.

Funding This work was supported by Russian Science Foundation, Grant No. 19-72-10030-P, https://rscf.ru/project/19-72-10030/.

Data availability All data generated in the presented experiment can be provided by authors in response to a reasonable request. In particular, we are ready to provide data if someone wants to repeat our experiment or if these data is considered useful for another research.

Declarations

Conflict of interest We declare no conflict of interest.

References

1. Lee, Y.J., Lee, J., Kim, K.K., Kim, Y.-B., Ayers, J.: Low power cmos electronic central pattern generator design for a biomimetic underwater robot. Neurocomputing **71**(1–3), 284–296 (2007). https://doi.org/10.1016/j.neucom.2006.12.013
2. Lodi, M., Shilnikov, A.L., Storace, M.: Design principles for central pattern generators with preset rhythms. IEEE Trans. Neural Netw. Learn. Syst. **31**(9), 3658–3669 (2020). https://doi.org/10.1109/TNNLS.2019.2945637
3. Kurkin, S.A., Kulminskiy, D.D., Ponomarenko, V.I., Prokhorov, M.D., Astakhov, S.V., Hramov, A.E.: Central pattern generator based on self-sustained oscillator coupled to a chain of oscillatory circuits. Chaos **32**(3), 033117 (2022). https://doi.org/10.1063/5.0077789
4. Scheffer, I.E., Berkovic, S., Capovilla, G., Connolly, M.B., French, J., Guilhoto, L., Hirsch, E., Jain, S., Mathern, G.W., Moshé, S.L., Nordli, D.R., Perucca, E., Tomson, T., Wiebe, S., Zhang, Y.-H., Zuberi, S.M.: Ilae classification of the epilepsies: position paper of the ilae commission for classification and terminology. Epilepsia **58**(4), 512–521 (2017). https://doi.org/10.1111/epi.13709
5. Cavalheiro, E.A.: The pilocarpine model of epilepsy. Ital. J. Neurol. Sci. **16**(1), 33–37 (1995). https://doi.org/10.1007/BF02229072
6. Coulter, D.A., McIntyre, D.C., Löscher, W.: Animal models of limbic epilepsies: What can they tell us? Brain Pathol. **12**(2), 240–256 (2002). https://doi.org/10.1111/j.1750-3639.2002.tb00439.x
7. Tagne, J.F., Edima, H.C., Njitacke, Z.T., Kemwoue, F.F., Mballa, R.N., Atangana, J.: Bifurcations analysis and experimental study of the dynamics of a thermosensitive neuron conducted simultaneously by photocurrent and thermistance. Eur. Phys. J. Spec. Top. **231**(5), 993–1004 (2022). https://doi.org/10.1140/epjs/s11734-021-00311-w
8. Kulminskiy, D.D., Ponomarenko, V.I., Prokhorov, M.D., Hramov, A.E.: Synchronization in ensembles of delay-coupled nonidentical neuronlike oscillators. Nonlinear Dyn. **98**(1), 735–748 (2019). https://doi.org/10.1007/s11071-019-05224-x
9. Egorov, N.M., Ponomarenko, V.I., Sysoev, I.V., Sysoeva, M.V.: Simulation of epileptiform activity using network of neuron-like radio technical oscillators. Tech. Phys. **66**(3), 505–514 (2021).https://doi.org/10.21883/JTF.2021.03.50532.237-20
10. Egorov, N.M., Ponomarenko, V.I., Melnikova, S.N., Sysoev, I.V., Sysoeva, M.V.: Common mechanisms of attractorless oscillatory regimes in radioengineering models of brain thalamocortical network. Izvestiya VUZ. Appl. Nonlinear Dyn. **29**(6), 927–942 (2021).https://doi.org/10.18500/0869-6632-2021-29-6-927-942
11. Egorov, N.M., Kulminskiy, D.D., Ponomarenko, V.I., Sysoev, I.V., Sysoeva, M.V.: Transient dynamics in electronic neuron-like circuits in application to modeling epileptic seizures. Nonlinear Dyn. (2022) (in press).https://doi.org/10.1007/s11071-022-07379-6
12. Kapustnikov, A.A., Sysoeva, M.V., Sysoev, I.V.: Modeling spike-wave discharges in the brain with small neu-

rooscillator networks. Math. Biol. Bioinform. **16**, 139–146 (2020).https://doi.org/10.17537/2020.15.138
13. Kapustnikov, A.A., Sysoeva, M., Sysoev, I.V.: Transient dynamics in a class of mathematical models of epileptic seizures. Commun. Nonlinear Sci. Numer. Simul. **109**, 106284 (2022). https://doi.org/10.1016/j.cnsns.2022.106284
14. Egorov, N.M., Sysoev, I.V., Ponomarenko, V.I., Sysoeva, M.V.: Epileptiform activity generation by an ensemble of complete electronic FitzHugh–Nagumo oscillators connected by a sigmoid couplings. In: Postnov, D.E., Khlebtsov, B.N. (eds.) Computational Biophysics and Nanobiophotonics, vol. 12194, p. 1219403. International Society for Optics and Photonics, SPIE, California (2022).https://doi.org/10.1117/12.2623993
15. Egorov, N.M., Sysoev, I.V., Ponomarenko, V.I., Sysoeva, M.: Complex regimes in electronic neuron-like oscillators with sigmoid coupling. Chaos, Solitons & Fractals **160**, 112171 (2022). https://doi.org/10.1016/j.chaos.2022.112171
16. Wang, Q., Perc, M., Duan, Z., Chen, G.: Impact of delays and rewiring on the dynamics of small-world neuronal networks with two types of coupling. Phys. A **389**(16), 3299–3306 (2010). https://doi.org/10.1016/j.physa.2010.03.031
17. Glyzin, S.D., Preobrazhenskaia, M.M.: Multistability and bursting in a pair of delay coupled oscillators with a relay nonlinearity. IFAC-PapersOnLine **52**(18), 109–114 (2019). https://doi.org/10.1016/j.ifacol.2019.12.215
18. Egorov, N.M., Sysoeva, M.V., Ponomarenko, V.I., Kornilov, M.V., Sysoev, I.V.: Ring generator of neuron-like activity with tunable frequency. Izvestiya VUZ. Appl. Nonlinear Dyn. **31**(1), 103–120 (2023).https://doi.org/10.18500/0869-6632-003025
19. Kuznetsov, Y.A.: Elements of Applied Bifurcation Theory. Springer, New York (2004).https://doi.org/10.1007/978-1-4757-3978-7
20. Gonchenko, S.V., Gonchenko, A.S., Kazakov, A.O., Kozlov, A.D., Bakhanova, Y.V.: Mathematical theory of dynamical chaos and its applications: review, part 2. Spiral chaos of three-dimensional flows. Izvestiya VUZ. Appl. Nonlinear Dyn. **27**(5), 7–52 (2019).https://doi.org/10.18500/0869-6632-2017-25-2-4-36
21. Rabinovich, M.I., Trubetskov, D.I.: Oscillations and Waves in Linear and Nonlinear Systems. Kluwer Academic Publisher, Dordrecht (1989).https://doi.org/10.1007/978-94-009-1033-1
22. Blekhman, I.I., Fradkov, A.L., Nijmeijer, H.H.J.C., Pogromsky, A.Y.: On self-synchronization and controlled synchronization. Syst. Control Lett. **31**(5), 299–305 (1997). https://doi.org/10.1016/S0167-6911(97)00047-9
23. Pikovsky, A., Rosenblum, M., Kurths, J., Synchronization, A.: Synchronization: A Universal Concept in Nonlinear Sciences. Cambridge University Press, London (2001)
24. Glyzin, S.D., Preobrazhenskaia, M.M.: Ring of unidirectionally synaptically coupled neurons with a relay nonlinearity. In: Advances in Neural Computation, Machine Learning, and Cognitive Research IV: Selected Papers from the XXII International Conference on Neuroinformatics, October 12–16, 2020, Moscow, Russia, pp. 347–356. Springer (2021).https://doi.org/10.1007/978-3-030-60577-3_41
25. Kornilov, M.V., Sysoev, I.V.: Mathematical model of a main rhythm in limbic seizures. Mathematics **11**(5), 1233 (2023). https://doi.org/10.3390/math11051233
26. Sysoev, I.V., Kornilov, M.V., Makarova, N.A., Sysoeva, M.V., Vinogradova, L.V.: Modeling limbic seizure initiation with an ensemble of delay coupled neuroscillator. In: Lacarbonara, W., Balachandran, B., Leamy, M.J., Ma, J., Machado, J.T., Stepan, G. (eds.) Advances in Nonlinear Dynamics, pp. 73–81. Springer, Cham (2022).https://doi.org/10.1007/978-3-030-81170-9_7
27. Paz, J.T., Huguenard, J.R.: Microcircuits and their interactions in epilepsy: Is the focus out of focus? Nat. Neurosci. **18**, 351–359 (2015). https://doi.org/10.1038/nn.3950
28. Linares-Barranco, B., Sánchez-Sinencio, E., Rodríguez-Vazquez, Á., Huertas, J.L.: A CMOS implementation of FitzHugh-Nagumo neuron model. IEEE J. Solid-State Circuits **26**(7), 956–965 (1991). https://doi.org/10.1109/4.92015
29. Folowosele, F., Hamilton, T.J., Etienne-Cummings, R.: Silicon modeling of the Mihalaş-Niebur neuron. IEEE Trans. Neural Netw. **22**, 1915–1927 (2011). https://doi.org/10.1109/tnn.2011.2167020
30. Binczak, S., Jacquir, S., Bilbault, J.-M., Kazantsev, V.B., Nekorkin, V.I.: Experimental study of electrical FitzHugh-Nagumo neurons with modified excitability. Neural Netw. **19**(5), 684–693 (2006). https://doi.org/10.1016/j.neunet.2005.07.011
31. Sobayo, T., Fine, A.S., Gunnar, E., Kazlauskas, C., Nicholls, D., Mogul, D.J.: Synchrony dynamics across brain structures in limbic epilepsy vary between initiation and termination phases of seizures. IEEE Trans. Biomed. Eng. **60**(3), 821–829 (2012). https://doi.org/10.1109/TBME.2012.2189113
32. Senhadji, L., Wendling, F.: Epileptic transient detection: wavelets and time-frequency approaches. Neurophysiol. Clin. **32**(3), 175–192 (2002). https://doi.org/10.1016/S0987-7053(02)00304-0
33. Patel, G.N., DeWeerth, S.P.: Analogue VLSI Morris-Lecar neuron. Electron. Lett. **33**(12), 997–998 (1997). https://doi.org/10.1049/el:19970686